COMPUTER METHODS AND PROGRAMS IN BIOMEDICINE 100 (2010) 39–48

journal homepage: www.intl.elsevierhealth.com/journals/cmpb

Distinguishing patients with celiac disease by quantitative analysis of videocapsule endoscopy images

Edward J. Ciaccio[a,*], *Christina A. Tennyson*[b], *Suzanne K. Lewis*[b], *Suneeta Krishnareddy*[b], *Govind Bhagat*[c], *Peter H.R. Green*[b]

[a] *Department of Pharmacology, Columbia University College of Physicians and Surgeons, United States*
[b] *Department of Medicine, Columbia University College of Physicians and Surgeons, United States*
[c] *Department of Pathology, Columbia University College of Physicians and Surgeons, United States*

ARTICLE INFO

Article history:
Received 13 August 2009
Received in revised form
31 January 2010
Accepted 22 February 2010

Keywords:
Celiac disease
Disease markers
Endoscopy
Small intestine
Videocapsule

ABSTRACT

Background: Although videocapsule endoscopy images are helpful in the evaluation of celiac disease, their interpretation is subjective. Quantitative disease markers could assist in determining the extent of villous atrophy and response to treatment.

Method: Capsule endoscopy images were acquired from celiac patients with small bowel pathology ($N = 11$) and from control patients ($N = 10$). Image resolution was 576×576 pixels in dimension, 256 grayscale levels, and had a $2\,s^{-1}$ frame rate. Pixel brightness and image texture were measured over 10×10 pixel subimages and then averaged for 56×56 subimages per frame. Measurements were obtained at five locations from proximal to distal small intestine in each patient. At each location, measurements were calculated using 200 consecutive image frames (100 s). Mean frame-to-frame pixel brightness, image texture, and periodicity in brightness, an estimate of wall motion or intestinal motility, were computed and used for classification with a nonlinear discriminant function.

Results: From pooled data, celiac images had greater texture than did images from control patients ($p < 0.001$) and exhibited more frame-to-frame brightness variation as well ($p = 0.032$). The dominant period of brightness was longer in celiacs ($p = 0.001$), possibly indicating decreased motility. Using the markers for three-dimensional nonlinear classification of celiacs versus controls, sensitivity was 92.7% and specificity was 93.5%. The relationship between dominant period and small intestinal transit time was approximately linear for both celiacs and controls ($r^2 = 0.42$ and $r^2 = 0.55$, respectively).

Conclusions: Videocapsule images can be quantified to detect villous atrophy throughout the small intestine, and to distinguish individuals with celiac disease from individuals lacking mucosal atrophy.

1. Introduction

Celiac disease (CD) is common, affecting about 1% of the population worldwide [1]. Diagnosis is made mainly through biopsies taken at endoscopic examination of the upper small intestine. There are several visual changes identified in the small intestine at standard video endoscopy and at videocapsule endoscopy that include villous atrophy, scalloping, fissuring, mucosal atrophy, layering or stacking of mucosal folds, and mosaic patterns [2], often in the proximal region but frequently also in the mid and distal small bowel [3,4].

* *Corresponding author at*: Celiac Disease Center at Columbia University Medical Center, 180 Fort Washington Avenue, New York, NY 10032, United States. Tel.: +1 212 305 5447; fax: +1 212 342 0447.
E-mail address: ciaccio@columbia.edu (E.J. Ciaccio).
0169-2607/$ – see front matter © 2010 Elsevier Ireland Ltd. All rights reserved.
doi:10.1016/j.cmpb.2010.02.005

Conventional endoscopy is not routinely used for imaging the mid and distal small intestine, however wireless videocapsule endoscopy is a noninvasive imaging method that can be used to evaluate the intestinal mucosa along the entire length of small bowel for evidence of CD, or its complications [4,5].

The videocapsule endoscopy camera produces high quality images of the small bowel mucosa at a rate of $2\,s^{-1}$ and is able to detect minute mucosal details, including changes in intestinal villi [6,7]. Videocapsule endoscopy is being used increasingly to assess patients with celiac disease, especially when they are unable, or unwilling to undergo standard endoscopy [5]. However, clinical scoring of these images is subjective and requires training. It is not always possible to visually discern subtle differences between videocapsule images, particularly in low contrast areas. If image processing could be used to automatically assess videocapsule images for presence of pathology, it would potentially be very useful as a clinical diagnostic tool.

2. Background

The types of visual features that are observed by gastroenterologists upon examination of videocapsule endoscopy images suggesting celiac disease include villous atrophy (68.1%), mucosal fissuring (61.7%), layering (40.4%), and mosaic pattern (19.1%), with changes extending into the ileum [8]. Videocapsule endoscopy has also proven useful to evaluate patients with known celiac disease who have ongoing symptoms or who develop alarm symptoms such as pain, fever, weight loss, or bleeding, despite adhering to a gluten-free diet [9,10]. Furthermore, videocapsule endoscopy can be used to diagnose, monitor, and assess for complications of CD [11] including those observed in patients with type II refractory celiac disease [12].

A major drawback of videocapsule endoscopy is that its sensitivity in detecting villous atrophy by visual inspection of the images alone ranges between 70% and 87.5%, while the specificity ranges between 100% and 90.9% [6,13,14]. The moderate agreement of the videocapsule findings of intestinal mucosal atrophy with the histologic pattern, despite resulting in a high specificity, has a lower sensitivity. Thus visual inspection of videocapsule endoscopy images by themselves cannot replace traditional biopsy examination [15], and for the purpose of diagnosing complications of celiac disease, videocapsule endoscopy has the status of a grade C recommendation [16]. In this study we report on the development of quantitative disease markers to detect pathology throughout the small bowel in celiac patients, compared to normal patients, which are readily applicable to videocapsule imaging.

3. Method

3.1. *Clinical*

Eleven celiac patients were studied, ten had biopsy changes characteristic of celiac disease (Marsh grades II–IIIC), while one patient had no biopsy performed because of hemophilia. Controls consisted of ten patients with normal histology being evaluated for other gastrointestinal complaints at the Columbia University Medical Center, New York from February 1, 2009 to December 31, 2009. All patients consented to videocapsule endoscopy study. The indication for capsule endoscopy in control patients included obscure bleeding and diarrhea. Patients with age under 18 years, pregnancy, history of intestinal obstruction, presence of a pacemaker, and chronic use of non-steroidal anti-inflammatory drugs (NSAIDs) were excluded from study. Only studies that reached the cecum were included for analysis.

The PillCam SB2 videocapsule (Given Imaging, Yoqneam, Israel) was used to obtain videocapsule endoscopy images. The system consists of a recorder unit, battery pack, antenna lead set, recorder unit harness, battery charger and recorder unit cradle. The capsule is 26 mm × 11 mm in size and has a frame rate of two digital images per second ($2\,s^{-1}$). All subjects swallowed the PillCam SB2 videocapsule after a 12-h fast with approximately 200 cc water and 80 mg simethicone. Subjects were allowed to drink water 2 h after ingesting the capsule and to eat a light meal after 4 h. The data recorder was worn on a belt by the patient and received radio image signals via a sensor array transmitted by the videocapsule as it passed through the GI tract. Capsule endoscopy images were recorded over an 8-h period. At the end of 8 h, the images were downloaded to a PC-based workstation. The videos were interpreted using Rapid5 software (Given Imaging, Yoqneam, Israel) by gastroenterologists, each with experience in reading over fifty capsule endoscopies. After marking the first duodenal image and cecal image, the total intestinal transit time was calculated for each videocapsule endoscopy study. De-identified videoclips of 200 frames each were acquired from five locations in the small intestine of each patient. The total small bowel transit time was divided into tertiles, corresponding to the proximal, mid and distal small bowel respectively. Videoclips were obtained from each tertile (locations 2–4), from the proximal duodenum as the capsule first entered the small bowel (location 1), and from the distal ileum (location 5). The videos were reviewed using proprietary software.

3.2. *Quantitative*

Videoclips created from patient data were transferred without patient identifiers to a dedicated PC type computer for quantitative analysis. From each videoclip, grayscale images (256 levels) with an image dimension of 576 × 576 pixels were extracted using Matlab Ver. 7.7, 2008 (Mathworks, Natick MA). The images were processed as follows. Subimages of 10 × 10 pixels were extracted from each image using computer software developed in-house (56 × 56 per image excluding borders). The average grayscale level (brightness) and the standard deviation in grayscale level (image texture) of each subimage were calculated and averaged for the image frame. The means and standard deviations over 200 frames (100 s) were then computed and tabulated. Over the 200 video frames, the standard deviation in brightness, i.e. the brightness variability, which reflected temporal changes, and the mean image texture, which reflected the localized spatial variability, were used as parameters for classification of each videoclip. Greater

brightness variability, and greater image texture, were hypothesized to be indicative of villous atrophy. The crevices and fissures that are a hallmark of villous atrophy at the macroscopic level are dark in color and would manifest as a greater variation in the grayscale level. Similarly, greater variability in brightness from frame-to-frame was hypothesized to be indicative of patchy villous atrophy, a hallmark of celiac disease. Videos in a few areas in some patients were excluded due to the lack of clarity when opaque extraluminal fluid and/or air bubbles were present. Videoclips having opaque extraluminal fluid or air bubbles comprising >10% of the area in image frames were excluded from further analysis. When lesser amounts of opaque extraluminal fluid or air bubbles, which have the capacity to magnify the surface texture, were present, they were considered as a first approximation to act as random noise for purposes of analysis. Both celiac and normal patients were found to have some opaque extraluminal fluid and air bubbles in portions of the image frames. For the 11 celiac patients a total of 55 videoclips, and for the 10 controls, a total of 50 videoclips were analyzed (one from each of five locations in each patient). Four of the 50 control videoclips were excluded from further analysis due to presence of opaque extraluminal fluid or air bubbles.

3.3. *Dominant period analysis*

To estimate wall motion, the dominant period of the brightness parameter was calculated over 200 frames. This was done using a procedure called dominant frequency analysis. The dominant frequency is defined as the fundamental frequency component with the greatest spectral power in the frequency range of interest [17,18] and it therefore provides a measurement of the most prevalent periodicity in the pattern of image intensity over time. Since the signal length of 200 frames was quite short, rather than use Fourier analysis, the calculation was done as follows [17,18]. The mean brightness value over 200 image frames was treated as a signal. The ensemble average vector $\underline{e}_w$ was obtained by averaging successive mean-zero signal segments of window length w:

$$\underline{e}_w = \left(\frac{1}{n}\right) \mathbf{U}_w \underline{s} \tag{1a}$$

$$\mathbf{U}_w = [\mathbf{I}_w\, \mathbf{I}_w \ldots \mathbf{I}_w] \tag{1b}$$

where $\underline{s}$ is the signal vector of length N, $\mathbf{I}_w$ are $w \times w$ identity submatrices, and the sequence is cropped so that the computation matrix $\mathbf{U}_w$ is $w \times N$ in dimension, and the number of summations for a signal window length (segment length) w is:

$$n = \text{int}\left(\frac{N}{w}\right) \tag{2}$$

The ensemble average energy is given by:

$$E_w = \underline{e}_w^T \underline{e}_w \tag{3}$$

And the root mean square power of the ensemble average is:

$$P_w = sqrt\left(\frac{E_w}{w}\right) \tag{4}$$

The ensemble average (EA) frequency spectrum is formed by plotting $sqrt(n) \times P_w$ versus w. The $sqrt(n)$ term is used to level the spectral brightness background across the spectrum, which would otherwise decrease with w by $1/sqrt(n)$, the degree of noise falloff per number of summations n used for ensemble averaging. The low spectral limit for analysis was selected as 40 sample points (20 s), and the high spectral limit was selected as 3 sample points (1.5 s). The dominant period of the EA spectrum was defined as the segment length w^* in seconds of the largest fundamental peak in the power spectrum [17,18]. The dominant period was also computed for temporal variability in texture, but for simplicity this was not included in subsequent calculations.

We then determined how well the quantitative markers extracted from each videoclip: brightness and its variation, texture, and dominant period of brightness, could be used for comparing and contrasting celiac versus control videoclips. The mean and standard deviation of pooled data from each area, and from all areas combined, was calculated in celiacs versus controls. The significance between means was determined using the unpaired t-test (SigmaPlot ver. 9.01, Systat Software, 2004) and the significance between the standard deviations was calculated using the F-test (Medcalc ver. 9.5, 2008). Scatterplots of the data were constructed. The best nonlinear discriminant boundary for classification of celiacs versus controls was determined manually in a three-dimensional scatterplot as projected into two dimensions. The feature distribution was then projected into eigenspace using Matlab for eigenvector computation (ver. 7.7, The Mathworks, 2008), and the best linear discriminant function for classification in eigenplane 1–2 was determined. We hypothesized that this eigenplane would provide the greatest separation between the two classes (celiac and control) since variance is maximized. The transit times for celiacs and controls were compared to their mean dominant periods in image brightness (locations 1–4) using linear regression analysis (SigmaPlot ver. 9.01, Systat Software, 2004).

4. Results

In Fig. 1 are shown example color images obtained from the videocapsule recorder at locations 4 and 2 in two normal (A–B) and locations 3 and 2 in two celiac patients (C–D). Both the villi and the mucosal folding patterns do not show any abnormality in the normal patients (panels A–B). However in the celiac patient images, a high degree of fissuring and scalloping of the edges was observed (panels C–D). These findings suggest that there will be a greater degree of spatial variability in terms of textural changes in the celiac images.

Quantitative markers of image brightness from a control patient (area 3) are shown in Fig. 2. The variation in mean image brightness over 200 frames (100 s) is shown in panel A. The mean brightness over this interval was 77.1 for a grayscale range of 1–256 (256 = brightest). A number of peaks and oscilla-

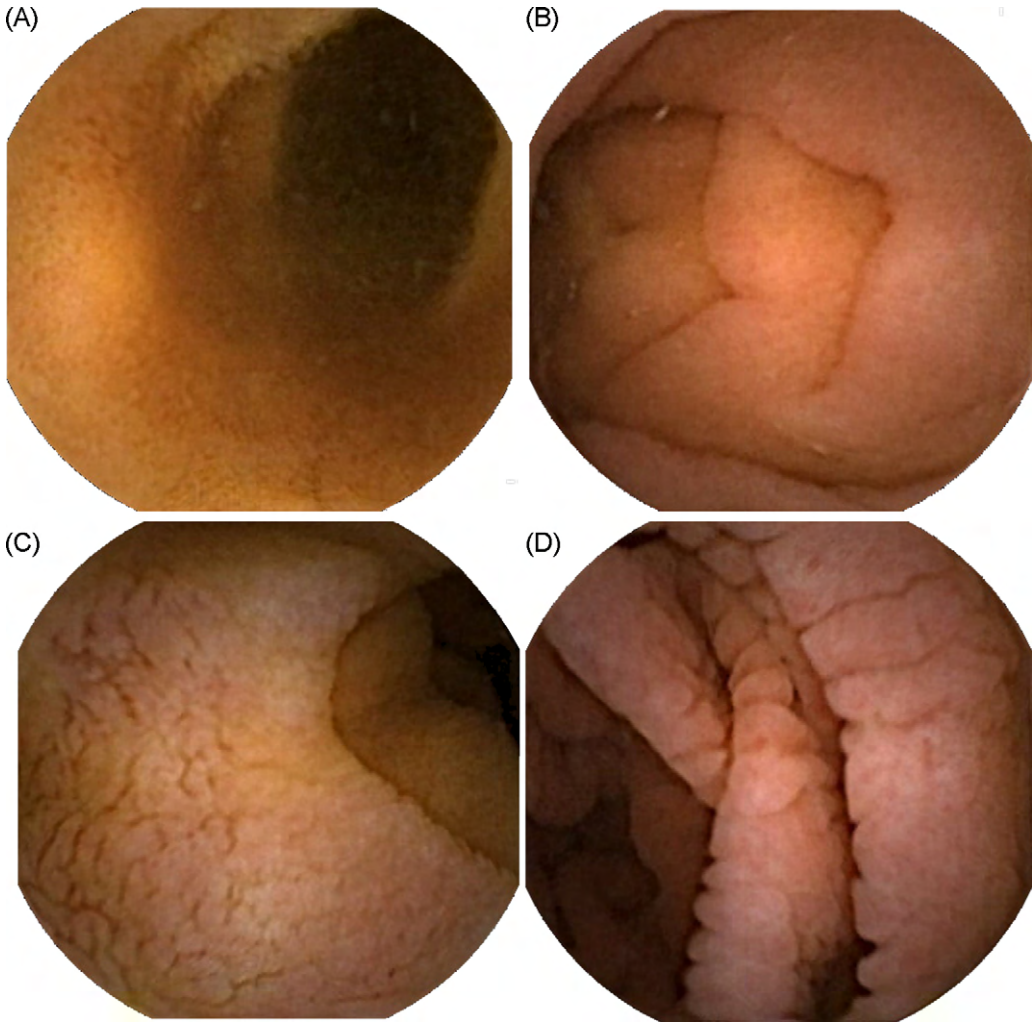

Fig. 1 – Color image frames acquired from the capsule video. Upper panels: Controls–luminal wall and folds. Lower panels: Celiacs–luminal wall and folds. These color images are transformed to 256 level grayscale images in ImageJ prior to further processing.

tions are evident. There appears to be a short range oscillation consisting of individual peaks as well as longer range oscillations consisting of clusters of peaks. The spectrum of the data from panel A is shown in panel B. There is a prominent peak at $w = 9$ sample points (4.5 s) as well as a secondary peak at $w = 26$–28, which may be the third harmonic (in which case the second harmonic is the smaller peak at $w = 18$). The temporal change in image texture for this normal patient is shown in panel C. The mean texture level is 8.4 grayscale. Peaks of variability (panel C) appear to have similar time duration as compared with peaks of brightness (panel A) and the quantitative spectrum of variability shows a dominant peak at 4.0 s (panel D), approximately the same as the dominant peak for brightness (panel C).

In Fig. 3 the same quantitative image markers are shown from a celiac patient (area 3). The mean brightness level (Fig. 3A) is lower in this celiac patient (65.0/256) as compared with the control patient (Fig. 2A). The dominant period in brightness is 6.5 s (Fig. 3B), substantially longer than that of the normal patient which is 4.5 s (Fig. 2B). The image texture has a mean value of 9.3 (Fig. 3C), which is higher than for the normal patient (8.4, Fig. 2C). The dominant period in variability was also long in this patient, 8 s (Fig. 3D).

The mean values for disease markers from all videoclips are provided in Table 1. The three markers used subsequently for classification of mucosal atrophy (brightness variability, image texture, and dominant period), had significantly different mean levels in celiacs versus controls based upon the unpaired *t*-test ($p = 0.032$, $p < 0.001$, $p = 0.001$, respectively). The brightness variability and image texture were significantly higher in celiacs indicating greater changes between neighboring regions and increased likelihood of pathology in these patients. The dominant period was longer in celiacs, which indicates a slower rate of periodic change as compared to control patients. The standard deviation of all features used for classification was significantly higher in celiacs versus controls based upon the *f*-test ($p \leq 0.001$ for all disease markers). This finding also indicates a greater quantitative variability in celiac patient images, as would be expected when pathology is present.

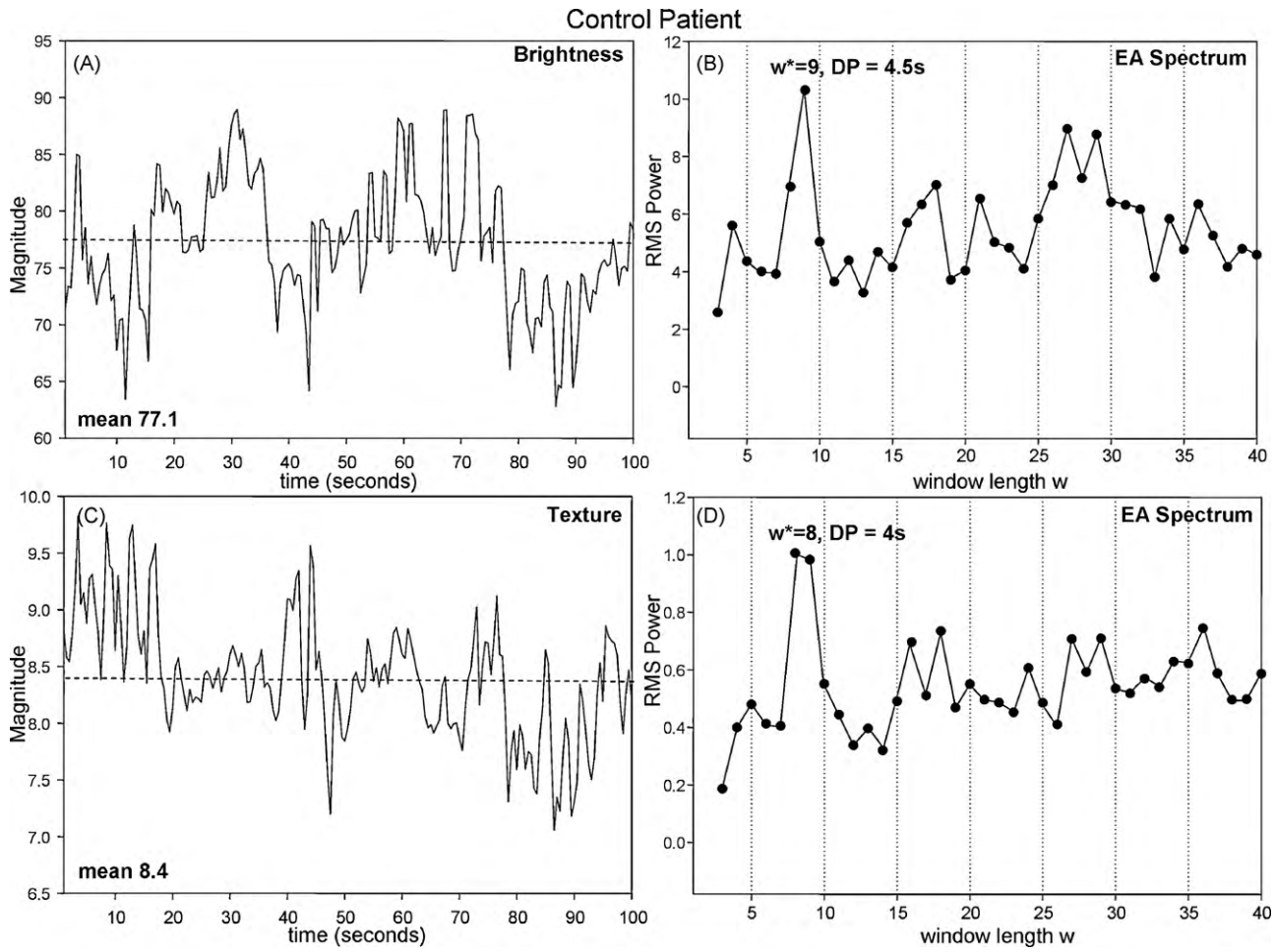

Fig. 2 – Quantitative markers from region 3 in control patient. (A) Trace of mean image brightness over 100 s (200 frames). (B) Spectral analysis of the panel A trace—the dominant period occurs at 4.5 s. (C) Trace of image texture over the same 100 s in the same patient (200 frames). (D) Spectral analysis of the panel C trace—the dominant period occurs at 4 s; however, this measurement is not used for further analysis.

The nonlinear boundary used for classification is shown in the scatterplot of Fig. 4 (dotted curved line) which was created with map3d, an interactive scientific visualization tool for bioengineering data (Scientific Computing and Imaging Institute, University of Utah) [19]. The X, Y, and Z axes represent brightness variability, dominant period, and image texture, respectively. The disease markers in control patients (blue) are clustered in a single area of the three-dimensional map. Many of the disease markers in celiac patients (red) are clustered away from the controls in every direction. The overall sensitivity and specificity are shown. The brightness of each color indicates its distance along the small intestine—darker blues and reds indicate images taken at more distal regions.

The distribution of Fig. 4 was projected onto eigenplane 1–2, which is the plane of greatest variance (Fig. 5). As compared with Fig. 4, there is a much greater spread between the points. The best linear discriminant function for separating celiacs from controls is shown. The sensitivity and specificity are almost 80%. The disease markers in control patients (blue) are mostly clustered at lower left. For celiac patients (red, and white) they are mostly clustered at upper right. The false negative celiac points (red, lower left) include all Marsh categories. The false positive control points (blue, upper right) are from different control patients.

Plots for mean values from each of the five areas of the small intestine are shown in Fig. 6. The celiac mean values are designated by solid circles and controls are designated by open circles. For all three disease markers at all five small intestinal regions, mean variation in image grayscale brightness is greater in celiacs than in controls (panel A), mean spatial variability or texture is greater in celiacs than in controls (panel B), and the mean dominant period of brightness is longer in celiacs than in controls (panel C). There was a significant difference between celiacs and controls for all three parameters using pooled data (Table 1).

A scatterplot showing the relationship between dominant period in brightness, and transit time through the small intestine is given in Fig. 7. The r^2 value for the celiac patients is 0.42, while for controls it is 0.55. Thus the dominant period is linearly correlated to transit time, and the slope of the linear regression line can be used as a rough estimate of the

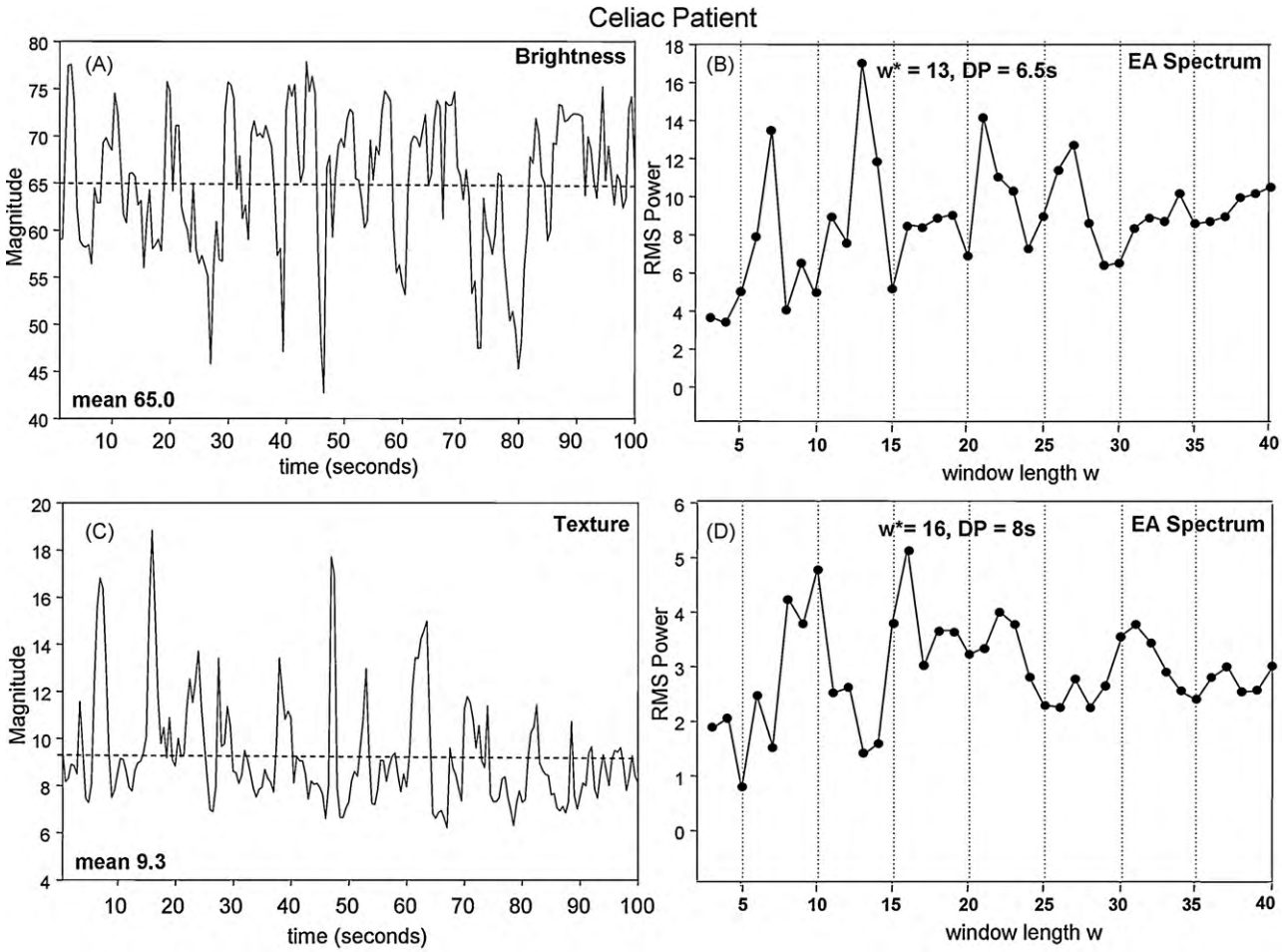

Fig. 3 – Quantitative markers from region 3 in celiac patient. Panels correspond to those in Fig. 2. (A) The brightness magnitude with mean value of 65.0 grayscale level. (B) Spectral content of A, with dominant period at 6.5 s. (C) Image texture with a mean value of 9.3 grayscale level. (D) Spectral content of C, with dominant period at 8 s.

relationship, which has a slightly different slope and different level in celiacs versus controls. The positive slope in both indicates that as transit time increases, so too does dominant period. The dominant period is indicative of the periodicity T of frame-to-frame image brightness, and therefore T is longer in celiac videoclips. In Fig. 7 the Marsh classifications of celiac patients, when known, are provided. In one celiac patient with hemophilia, a biopsy was not taken (marked with x).

5. Discussion

This study has implications for detection and assessment of celiac disease. From pooled data, images from celiac patients were more variable in terms of both brightness and texture, indicating greater differences in the pattern along the small intestinal lumen per frame and over time (from frame-to-frame). Standard deviations of these markers were

Table 1 – Summary of capsule image quantitative measurements.

Feature	Celiacs ($N = 11$)	Controls ($N = 10$)	t-Test	f-Test
Brightness (gsl)	71.8 ± 5.2	71.7 ± 4.2	NS	NS
Brightness variability (gsl)	1.3 ± 0.9	0.9 ± 0.4	$p = 0.032$	$p < 0.001$
Image texture (gsl)	8.7 ± 1.7	7.8 ± 1.0	$p < 0.001$	$p < 0.001$
Dominant period (s)	6.4 ± 2.6	4.7 ± 1.6	$p = 0.001$	$p = 0.001$

Data is shown as mean ± standard deviation. *t*-Test—significant difference in the means based on the unpaired *t*-test. *f*-Test—significant difference in the variances based on this test. NS = not significant, gsl = grayscale level.

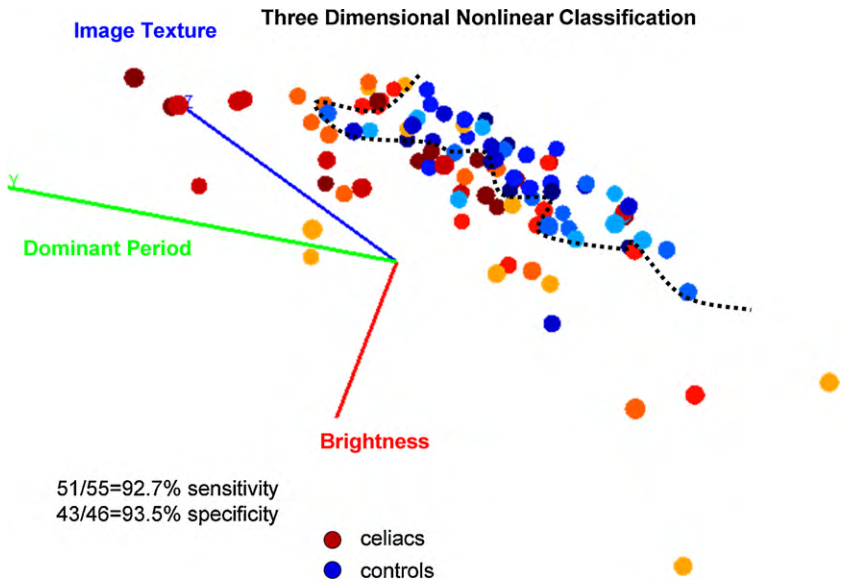

Fig. 4 – Best three-dimensional nonlinear classification of celiacs versus controls using brightness, dominant period and image texture as quantitative markers. The sensitivity and specificity for detecting celiac disease image sequences are shown. Light to dark color indicates small intestinal level from 1 to 5.

significantly higher in celiacs based on the f-test ($p \leq 0.001$, Table 1), again indicating greater variability.

The dominant period of brightness was longer in celiacs ($p = 0.001$, Table 1), possibly indicating decreased motility. The relative lack of anatomic attachments of the jejunum and ileum allow for complex motion [20]. The duodenum, however, is relatively fixed. Complex wall motion may in part be responsible for random variations in brightness that are evident in Figs. 2A and 3A (location 3, i.e. the mid-small bowel). Young people, normal volunteers, and Crohn's disease patients tend to have significantly shorter videocapsule endoscopy small bowel transit times that are indirectly influenced by gastric emptying [21]. In celiac disease a mean small bowel transit time of 4:43 ± 1:31 h has been observed versus 3:56 ± 1:22 h for healthy volunteers [21]. The measurement of a longer transit time in celiacs is in accord with the present study in which a longer dominant period, possibly indicative of reduced motility, was found in the celiac group.

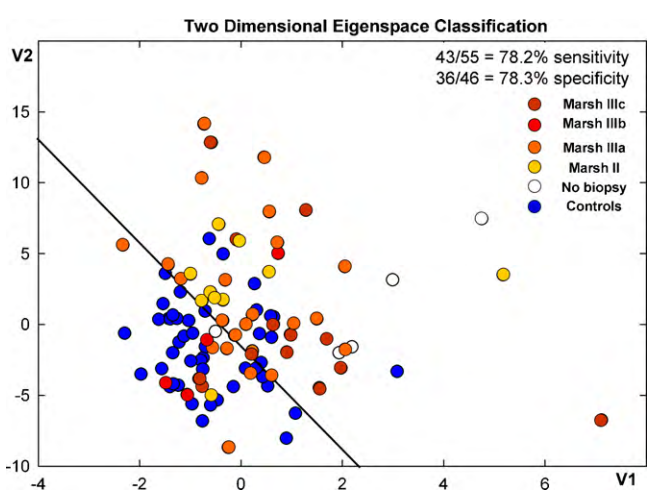

Fig. 5 – Projection of the distribution of Fig. 4 onto eigenplane 1–2. Eigenvectors V1 and V2 are unitless. The best linear discriminant function for classification of celiac versus control image sequences is denoted by a straight line. The process is automatable, and classification can potentially be improved by adding features. Marsh score is shown for celiac patient data.

We also assessed the degree of intestinal involvement in patients with celiac disease. We demonstrated in this study that abnormal videocapsule imagery can extend throughout the small intestine in celiac patients. In Fig. 6, mean brightness variability is higher, mean image texture is greater, and dominant period is longer in the celiac images as compared to controls at all small intestinal regions. This is consistent with previous studies of the distribution of villous atrophy in celiac disease. Traditionally the most severe histopathologic changes are found in the duodenum and upper jejunum in celiac disease, however the changes may involve a variable length of the small intestine [22] in regions not accessible to conventional upper GI endoscopy [7]. In some patients studied by capsule endoscopy the duodenum was not involved [11,23]. Jejunal inflammation can be detected during assessment of celiac patients using videocapsule endoscopy [24]. The inflammatory and atrophic processes can also involve the ileum in up to one third of patients as determined by inspection of videocapsule images and ileal biopsy [24,25]. Thus, we would anticipate presence of abnormal values for disease markers in the jejunum and ileum of many celiac patients as we identified. There is no correlation between the extent of small intestinal abnormality as determined by visual inspection of videocapsule endoscopy images and patient symptoms, especially diarrhea, a common symptom of untreated celiac disease [22]. The significance of the variable length of involvement of the intestine in patients with celiac disease is currently unclear but may be clarified in part

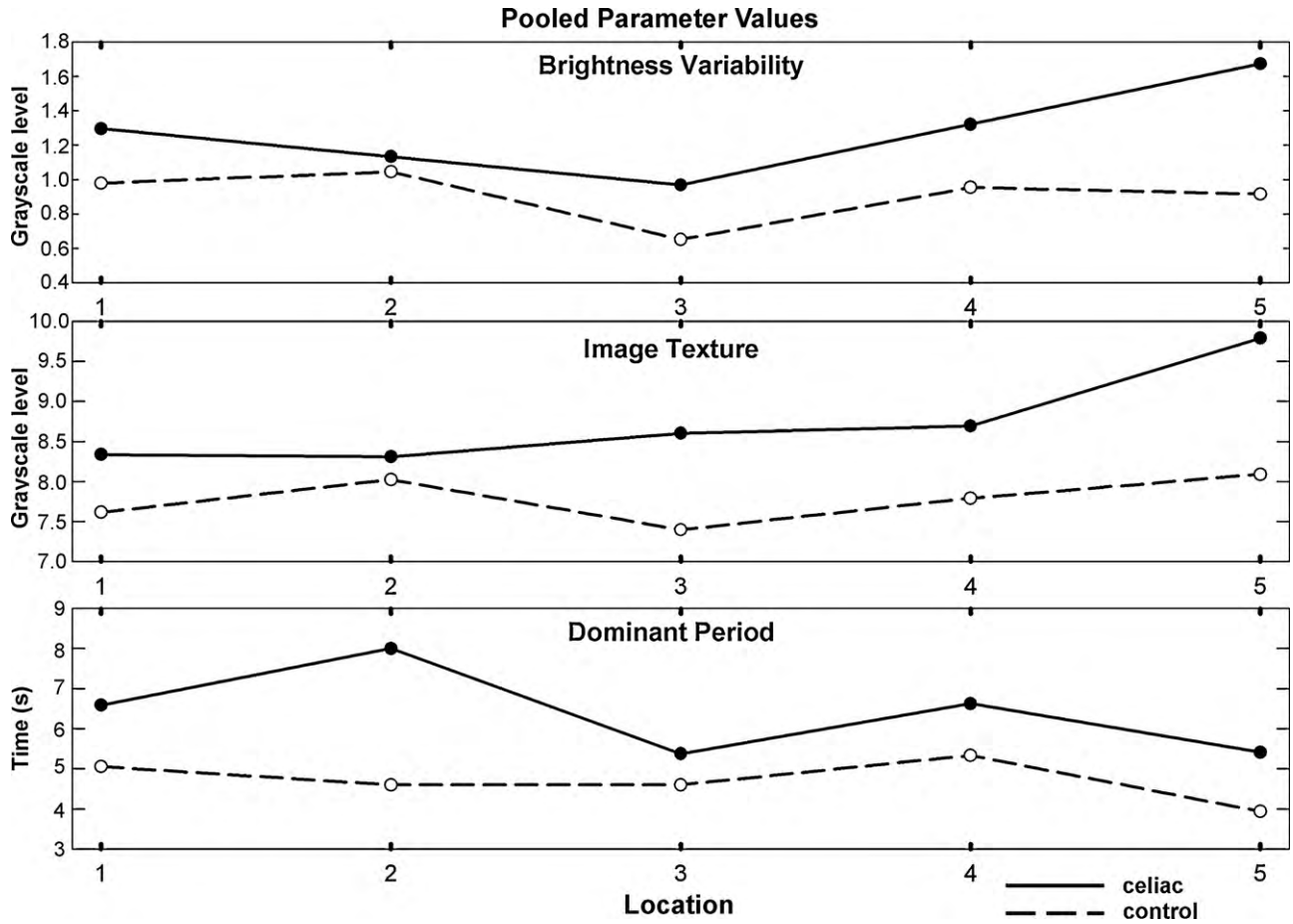

Fig. 6 – Plots of mean quantitative marker characteristics in regions 1–5. There is a significant difference between pooled celiac versus control values for all three markers (see Table 1). There is greater brightness variability and greater image texture in celiacs as compared with controls, and the dominant period is longer in celiacs.

through the use of quantitative disease markers. Furthermore, healing after onset of a gluten-free diet is thought to occur from the distal end upwards, suggesting the possibility to use the described quantitative markers as evidence of the efficacy of a gluten-free diet. This may be of great value in the assessment of drug therapy for celiac disease.

As an alternative to quantifying disease markers, clinical scoring of videocapsule endoscopy is subjective with limited resolution and thus can be problematic [7,13]. However the subjective nature of capsule endoscopy can be obviated by application of our quantitative techniques. Relative weaknesses of our study include a limited number of cases evaluated, and in this pilot study, selection of celiac patients with villous atrophy (Marsh II or III lesions). When patients with lesser degrees of villous atrophy are included, the correlation between the videocapsule endoscopy score and the histologic score might diminish [15]. Visual inspection of videocapsule endoscopy images may not be helpful to reliably recognize mild degrees of villous atrophy. Often, evaluation of capsule findings is performed by a single observer, thus the reproducibility and reliability in evaluating capsule findings in celiac disease is not yet clarified. If videocapsule endoscopy is to be used as a routine diagnostic tool for the diagnosis and follow-up of celiac disease, the ability of videocapsule endoscopy to recognize milder degrees of villous atrophy must be assessed.

To discern celiac disease image sequences from controls, we presented a three-dimensional nonlinear classifier method. This classifier was used regardless of where in the small intestine the images were being recorded from. Other limitations include the relatively short segments of video used for image analysis relative to the total intestinal transit time. Celiac disease may also be patchy [26] and the segments examined may not be representative due to sampling error. In future studies when a greater number of subjects are included, the resulting greater resolving power will enable more accurate threshold identification for classifying villous atrophy versus normal images at all small intestinal locations. Eigenanalysis is also a useful method to characterize data distributions based on their most variable components [27,28]. By definition, after reordering the eigenvectors according to eigenvalue magnitude, the distribution variance is maximized along eigenvectors 1 and 2 and therefore along eigenplane 1–2. Hence, projection onto this eigenplane maximally separates the points in the distribution. Using a linear discriminant function, it was possible to distinguish celiac from control small bowel image sequences with a sensitivity and specificity of almost 80% (Fig. 5). Although similar sensitivity and speci-

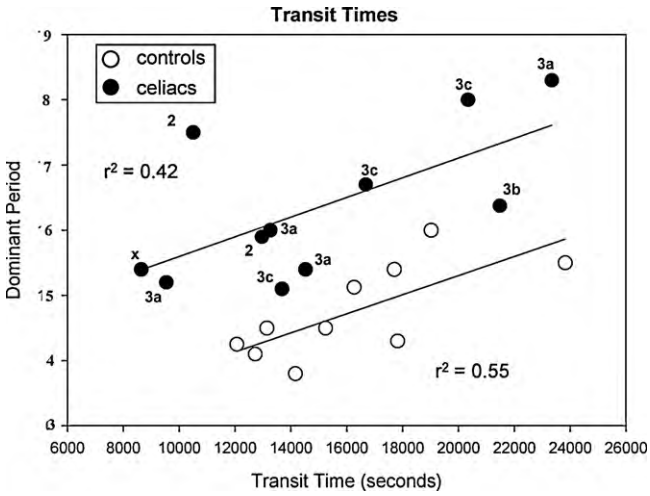

Fig. 7 – Scatterplot showing the relationship between dominant period and transit time in celiacs and controls. The linear regression lines are shown along with their r^2 values. The fit of celiac dominant period to transit time is $r^2 = 0.42$, and for controls $r^2 = 0.55$. The Marsh score for the individual patients is shown on the Graph. One celiac patient had hemophilia and was not biopsied (marked with x).

ficity might be obtainable by using linear discriminant analysis in the plane of Fig. 4, that plane was determined manually and somewhat tediously, whereas eigenplane 1–2 is determinable automatically. Were additional features to be added, projection of the distribution onto eigenplane 1–2 followed by linear discriminant analysis may yield improved automated classification, the subject of future work.

In this study, quantitative disease markers were developed to indicate presence of villous atrophy and abnormalities in motility from sequences of videocapsule images of the small intestine. Celiac patients were found to have greater quantitative variations in videocapsule images, both temporally (frame-to-frame brightness variability) and spatially (texture across the image) as compared to control patients (Table 1), suggesting the presence of pathology (villous atrophy) in celiacs. Such pathology is manifested as fissures and mucosal scalloping, that appears darker and more varied in texture as compared with areas having normal villi (Fig. 1). The periodicity of pixel brightness was found to be significantly longer in celiacs (Table 1), which suggests lesser motility in all areas of the small intestine. The three quantitative markers had a significantly greater standard deviation in celiacs, again suggesting that highly varied changes in image texture are indicative of pathology (Table 1).

The quantitative features that were developed were found to be useful to distinguish videocapsule images obtained in celiac patients versus those of control patients (Figs. 4 and 5). This distinctiveness in quantitative features occurred in all portions of the small intestine (Fig. 4). Furthermore, there appears to be no significant relationship between lesion severity and ability to classify an image sequence (Fig. 5). It is therefore possible to use this method prospectively to screen for celiac disease, to determine the degree of pathology throughout the small intestine, to determine change or improvement in the visual appearance in the same patient at different times, and to study the effect of a gluten-free diet or the effects of medications in celiac patients. Application of these image analysis techniques as well as other quantitative methods such as discriminant Fourier filters [29] can potentially enhance and extend the usefulness of videocapsule endoscopy.

Acknowledgements

The implementation of this study was made possible in part with a grant from the Celiac Sprue Association Peer Review Research Grant Program, and by software from the NIH/NCRR Center for Integrative Biomedical Computing, P41-RR12553-10.

REFERENCES

[1] P.H. Green, C. Cellier, Celiac disease, N. Engl. J. Med. 357 (2007) 1731–1743.
[2] S.K. Lee, P.H. Green, Endoscopy in celiac disease, Curr. Opin. Gastroenterol. 21 (2005) 589–594.
[3] P.H. Green, M. Rubin, Capsule endoscopy in celiac disease: diagnosis and management, Gastrointest. Endosc. Clin. N. Am. 16 (2006) 307–316.
[4] O. Ersoy, E. Akin, S. Ugras, S. Buyukasik, E. Selvi, G. Güney, Capsule endoscopy findings in celiac disease, Dig. Dis. Sci. 54 (2009) 825–829.
[5] C. Cellier, P.H. Green, P. Collin, J. Murray, ICCE consensus for celiac disease, Endoscopy 37 (2005) 1055–1059.
[6] R. Petroniene, E. Dubcenco, J.P. Baker, C.A. Ottaway, S.J. Tang, S.A. Zanati, C.J. Streutker, G.W. Gardiner, R.E. Warren, K.N. Jeejeebhoy, Given capsule endoscopy in celiac disease: evaluation of diagnostic accuracy and interobserver agreement, Am. J. Gastroenterol. 100 (2005) 685–694.
[7] E. Rondonotti, F. Villa, C.J. Mulder, M.A. Jacobs, R. de Franchis, Small bowel capsule endoscopy in 2007: indications, risks and limitations, World J. Gastroenterol. 13 (2007) 6140–6149.
[8] A. Culliford, J. Daly, B. Diamond, M. Rubin, P.H. Green, The value of wireless capsule endoscopy in patients with complicated celiac disease, Gastrointest. Endosc. 62 (2005) 55–61.
[9] P.H. Green, Mortality in celiac disease, intestinal inflammation, and gluten sensitivity, J. Am. Med. Assoc. 302 (2009) 1225–1226.
[10] O.M. Jolobe, Further indications for capsule endoscopy, South Med. J. 101 (2008) 1070.
[11] A. Muhammad, C.S. Pitchumoni, Newly detected celiac disease by wireless capsule endoscopy in older adults with iron deficiency anemia, J. Clin. Gastroenterol. 42 (2008) 980–983.
[12] S. Daum, U. Wahnschaffe, R. Glasenapp, M. Borchert, R. Ullrich, M. Zeitz, S. Faiss, Capsule endoscopy in refractory celiac disease, Endoscopy 39 (2007) 455–458.
[13] A.D. Hopper, R. Sidhu, D.P. Hurlstone, M.E. McAlindon, D.S. Sanders, Capsule endoscopy: an alternative to duodenal biopsy for the recognition of villous atrophy in coeliac disease? Dig. Liver Dis. 39 (2007) 140–145.
[14] E. Rondonotti, C. Spada, D. Cave, M. Pennazio, M.E. Riccioni, I. De Vitis, D. Schneider, T. Sprujevnik, F. Villa, J. Langelier, A. Arrigoni, G. Costamagna, R. de Franchis, Video capsule enteroscopy in the diagnosis of celiac disease: a multicenter study, Am. J. Gastroenterol. 102 (2007) 1624–1631.

[15] F. Biagi, E. Rondonotti, J. Campanella, F. Villa, P.I. Bianchi, C. Klersy, R. de Franchis, G.R. Corazza, Video capsule endoscopy and histology for small-bowel mucosa evaluation: a comparison performed by blinded observers, Clin. Gastroenterol. Hepatol. 4 (2006) 998–1003.
[16] R. Sidhu, D.S. Sanders, A.J. Morris, M.E. McAlindon, Guidelines on small bowel enteroscopy and capsule endoscopy in adults, Gut 57 (2008) 125–136.
[17] E.J. Ciaccio, A.B. Biviano, W. Whang, A.L. Wit, H. Garan, J. Coromilas, New methods for estimating local electrical activation rate during atrial fibrillation, Heart Rhythm 6 (2009) 21–32.
[18] E.J. Ciaccio, A.B. Biviano, W. Whang, A.L. Wit, J. Coromilas, H. Garan, Optimized measurement of activation rate at left atrial sites with complex fractionated electrograms during atrial fibrillation, J. Cardiovasc. Electrophysiol. 21 (2010) 133–143.
[19] R.S. MacLeod, C.R. Johnson, Map3d: interactive scientific visualization for bioengineering data, in: IEEE Engineering in Medicine and Biology Society 15th Annual International Conference, IEEE Press, New York, NY, 1993, pp. 30–31.
[20] A.K. Singh, R.M. Tierney, D.A. Low, P.J. Parikh, R.J. Myerson, J.O. Deasy, C.S. Wu, G.C. Pereira, S.H. Wahab, S. Mutic, P.W. Grigsby, A.J. Hope, A prospective study of differences in duodenum compared to remaining small bowel motion between radiation treatments, Rad. Oncol. 1 (2006) 1–5.
[21] Z. Fireman, Y. Kopelman, S. Friedman, H. Ephrath, E. Choman, H. Debby, R. Eliakim, Age and indication for referral to capsule endoscopy significantly affect small bowel transit times: the given database, Dig. Dis. Sci. 52 (2007) 2884–2887.
[22] P.H. Green, M. Rubin, Capsule endoscopy in celiac disease, Gastrointest. Endosc. 62 (2005) 797–799.
[23] J.A. Murray, A. Rubio-Tapia, C.T. Van Dyke, D.L. Brogan, M.A. Knipschield, B. Lahr, A. Rumalla, A.R. Zinsmeister, C.J. Gostout, Mucosal atrophy in celiac disease: extent of involvement, correlation with clinical presentation, and response to treatment, Clin. Gastroenterol. Hepatol. 6 (2008) 186–193, quiz 125.
[24] R. Makins, C. Blanshard, Guidelines for capsule endoscopy: diagnoses will be missed, Aliment. Pharmacol. Ther. 24 (2006) 293–297.
[25] W. Dickey, D.F. Hughes, Histology of the terminal ileum in coeliac disease, Scand. J. Gastroenterol. 39 (2004) 665–667.
[26] E.J. Ciaccio, G. Bhagat, A.J. Naiyer, L. Hernandez, P.H. Green, Quantitative assessment of the degree of villous atrophy in patients with coeliac disease, J. Clin. Pathol. 61 (2008) 1089–1093.
[27] E.J. Ciaccio, S.M. Dunn, M. Akay, A.L. Wit, J. Coromilas, C.A. Costeas, Localized spatial discrimination of epicardial conduction paths after linear transformation of variant information, Ann. Biomed. Eng. 22 (1994) 480–492.
[28] E.D. Angelini, E.J. Ciaccio, Optimized region finding and edge detection of knee cartilage surfaces from magnetic resonance images, Ann. Biomed. Eng. 31 (2003) 336–345.
[29] A. Vécsei, T. Fuhrmann, M. Liedlgruber, L. Brunauer, H. Payer, A. Uhl, Automated classification of duodenal imagery in celiac disease using evolved Fourier feature vectors, Comput. Methods Programs Biomed. 95 (Suppl. 1) (2009) S68–S78.